Available online at www.sciencedirect.com

ScienceDirect

journal homepage: www.elsevier.com/locate/he

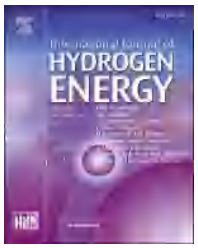

Enhanced hydrogen desorption/absorption properties of magnesium hydride with CeF_3@Gn

Ting He [a], *Xinhua Wang* [a,*], *Haizhen Liu* [b,**], *Shichao Gao* [a], *Yuanyuan Wang* [a], *Shouquan Li* [a], *Mi Yan* [a,***]

[a] *State Key Laboratory of Silicon Materials, School of Materials Science & Engineering, Zhejiang University, Hangzhou, 310027, China*

[b] *Guangxi Colleges and Universities Key Laboratory of Novel Energy Materials and Related Technology, Guangxi Novel Battery Materials Research Center of Engineering Technology, School of Physical Science and Technology, Guangxi University, Nanning, 530004, PR China*

HIGHLIGHTS

- Graphene and CeF_3 co-catalyzed MgH_2 were prepared by wet method ball milling and hydriding.
- Onset hydrogen desorption temperature decreased by 86 °C after co-addition of CeF_3@Gn.
- The maximum hydrogen desorption rates promoted 118 times at 200 °C.
- No eminent cycling degradation occurred after 15 hydrogen desorption/absorption cycles.

ARTICLE INFO

Article history:
Received 23 February 2019
Received in revised form
2 December 2019
Accepted 9 December 2019
Available online 6 January 2020

Keywords:
Hydrogen storage materials
Hydrogen storage properties
Magnesium hydride
Graphene
Catalysts

ABSTRACT

In order to improve the hydrogen storage performance of MgH_2, graphene and CeF_3 co-catalyzed MgH_2 (hereafter denoted as MgH_2+CeF_3@Gn) were prepared by wet method ball milling and hydriding, which is a simple and time-saving method. The effect of CeF_3@Gn on the hydrogen storage behavior of MgH_2 was investigated. The experimental results showed that co-addition of CeF_3@Gn greatly decreased the hydrogen desorption/absorption temperature of MgH_2, and remarkably improved the dehydriding/hydriding kinetics of MgH_2. The onset hydrogen desorption temperature of Mg + CeF_3@Gn is 232 °C , which is 86 °C lower than that of as-milled undoped MgH_2, and its hydrogen desorption capacity reaches 6.77 wt%, which is 99% of its theoretical capacity (6.84 wt%). At 300 °C and 200 °C the maximum hydrogen desorption rates are 79.5 and 118 times faster than that of the as-milled undoped MgH_2. Even at low temperature of 150 °C, the dedydrided sample (Mg + CeF_3@Gn) also showed excellent hydrogen absorption kinetics, it can absorb 5.71 wt % hydrogen within 50 s, and its maximum hydrogen absorption rate reached 15.0 wt% H_2/min, which is 1765 times faster than that of the undoped Mg. Moreover, no eminent degradation of hydrogen storage capacity occurred after 15 hydrogen desorption/absorption cycles. Mg + CeF_3@Gn showed excellent hydrogen de/absorption kinetics because of the MgF_2 and CeH_{2-3} that are formed in situ, and the synergic catalytic effect of these by-products and unique structure of Gn.

* *Corresponding author.*
** *Corresponding author.*
*** *Corresponding author.*
E-mail addresses: xinhwang@zju.edu.cn (X. Wang), lhzju@qq.com (H. Liu), mse_yanmi@zju.edu.cn (M. Yan).

https://doi.org/10.1016/j.ijhydene.2019.12.111

Introduction

Hydrogen energy is regarded as one of the most promising options to replace traditional energy because water is the only dominating combustion product which is clean and non-toxic. Solid-state storage of hydrogen has attracted extensive interest for on-board system because hydrogen in the form of hydrides which can offer high hydrogen density, safety and efficient mode of storage [1–5]. Among all hydrogen storage materials, MgH_2 is a very promising candidate for on-board applications due to its high gravimetric and volumetric capacity (7.6 wt% and 110 g/L, respectively), excellent reversibility, abundance and low cost. However, MgH_2 has its own shortcomings such as high desorption temperature and poor hydrogen absorption/desorption kinetics which hinders the practical application of MgH_2. How to resolve these problems has been a hot spot in the research of Mg-based hydrogen storage materials.

Various approaches have been presented and certified helpful for the design and synthesis of magnesium hydrogen storage system, such as alloying with other elements [6–9], nanosizing [10–12], adding catalysts/additives [13–16], mixing with various hydrogen storage materials [17–20], dielectric barrier discharge plasma assisted milling [21–23] have been reported and so on. In particular, many experiments have proved that adding catalysts is quite effective for reducing the operating temperature and improving the dehydrogenation kinetics of MgH_2. Among these, adding catalysts has been recognized to be a very effective method to reduce the onset and peak decomposition temperature, enhance the hydriding/dehydriding kinetics, and improve the reversibility of MgH_2 [24–29]. Mixing of MgH_2 with various metal halides is an effective strategy to improve the hydrogen sorption kinetics of Mg-based materials [30–35]. Ismail [35] studied the catalytic properties of $FeCl_3$ on hydrogen desorption kinetics of MgH_2, and displayed that the average dehydrogenation rate is 5–6 times faster than that of the undoped MgH_2. And MgH_2 powder with various transition metal halides shows favorable dehydrogenation performance, and they can release hydrogen at 225 °C [30]. Kumar et al. [33] reported that VCl_3 can in-situ generate metallic vanadium during ball milling along with MgH_2, and the material can absorb hydrogen even at room temperature. Ismail et al. [36] found that $CeCl_3$ can improve hydrogen storage properties of MgH_2 and active species are in situ formed Ce–Mg alloy, $MgCl_2$, and $CeH_{2.73}$.

Plentiful studies have suggested that the agglomeration of additive/catalyst is main reason for degradation in reversibility [37], and a lot of researches have shown that carbon structures can shorten hydrogen diffusion gateways and hinder the grain growth of MgH_2 during hydrogen sorption cycling [38–43]. Liu et al. [41,42] investigated few-layer graphene nanosheets in enhancing the hydrogen sorption kinetics of MgH_2, experimental results showed that MgH_2–5GNSs can absorb 6.6 wt% H_2 within 1 min and release 6.3 wt% H_2 within 80 min at 300 °C, and the hydrogen storage capacity has no difference after 6 desorption/absorption cycles. They believed that graphene nanosheets can provide more edge sites and hydrogen diffusion channels. Analogously, Singh et al. [38] proved that the presence of graphene can weaken the Mg–H bond, which is beneficial to reduce the hydrogen desorption temperature. MgH_2 mechanical milling with 5 wt% CNT can adsorb 0.059 g (H_2)/g (MgH_2) at 673 K and 4.6 MPa [16]. Soni et al. [39] synthesized MgH_2: CeF_4@Gr by direct ball milling commercial MgH_2 with CeF_4@Gr, the results of which showed that the dehydrogenation reaction with a total release of about 5.85 wt% of hydrogen and MgH_2:CeF_4@Gr absorbs 5.50 wt% hydrogen within 2.5 min at 300 °C under 1.5 MPa H_2 pressure. Zhang et al. [40] used the hydriding combustion synthesis and mechanical milling method to prepare Mg-based composites, and revealed the reason why the Mg@Ni/Gn composites have remarkable enhancement of hydrogen sorption kinetics is that in situ formed nanosized Mg_2NiH_4. The metal halide-carbon based co-doped is one of the key point in this hydrogen storage [34,44–46]. Ismail et al. [44] found the dopants of 10 wt% K_2NbF_7–5 wt% MWCNT have markedly reduced the initial decomposition temperature and decomposition activation energy of MgH_2, and the experiment proved that the by-product of MgF_2, KH, and Nb together with the unique structure of MWCNT are the active species to enhance the hydrogen storage properties of MgH_2.

Our recent research also revealed that the initial hydrogen desorption temperature is about 214 °C and maximum dehydriding rate is 572 times faster than that of commercial MgH_2 which exhibits remarkably thermodynamics and kinetics properties [47]. The studies carried out in our group have shown that MgH_2 can react with CeF_3 to in-situ generate MgF_2 and CeH_{2-3}, which are conducive to reduce hydrogen desorption temperature and improve hydrogen desorption/absorption kinetics of MgH_2 [48].

Various studies have shown that metal halides have good catalytic performance, which exhibits remarkably expedite hydrogen desorption/absorption kinetics. But most of them were focused on transition metal halides, reports on rare-earth metal halides are very few [49–52]. In this work, we attempted to introduce CeF_3/Graphene nanoplatelets (the mass ratio of CeF_3 to Gn is 7:3) to achieve the simultaneous enhancement of the hydrogen desorption/absorption thermodynamics and kinetics of MgH_2. To the best of my knowledge, up to now there have been no investigation of Mg + CeF_3@Gn. For the sake of contrast, Mg + Gn, Mg + CeF_3 and undoped Mg were prepared under the same conditions. It is found that co-addition of CeF_3@Gn greatly decreased the hydrogen desorption/absorption temperature of MgH_2, and remarkably improved the dehydriding/hydriding kinetics of MgH_2.

Experimental

Original powders of Mg (Sinopharm Croup, >99.0% in purity and 100–200 mesh in size), CeF_3 (Sinopharm Group, 99.9% in purity) were used as received. Graphene nanoplatelets (TCI, 6–8 nm in thickness and 15 μm in width) were treated with concentrated nitric acid (Sinopharm Group, GR, 65.0–68.0%),

anhydrous ether and tetrahydrofuran (Sinopharm Group, AR, ≥99.7%) as solvent.

Graphene nanoplates (250 mg) were incipiently treated with concentrated nitric acid (60 mL) by ultrasonication for 2 h at 40 kHz frequency to introduce functional groups, which is beneficial for other samples to load on its surface [40]. Followed by centrifugal washing and drying at 70 °C, the treated-graphene nanoplates and CeF_3 (30 wt%:70 wt%) were dispersed into 50 mL tetrahydrofuran by ultrasonication for 2 h at 40 kHz frequency, then dried at 70 °C, and the resulting sample is denoted as CeF_3@Gn.

Afterwards, 90 wt% Mg and 10 wt% CeF_3@Gn are mixed in anhydrous ether by ultrasonic dispersion for about 40 min, which allows the sample to dry naturally, during this process, the necessary anti-oxidation measures is indispensable. After grinding by hand for about 30 min, the powders were heated from room temperature to 350 °C to absorb hydrogen at a heating rate of 10 °C/min under 5 MPa hydrogen pressure for 10 h. Then these samples were prepared by ball milling using a QM-3SP4 planetary mill (Nanjing Nanda Instrument Plant) at 400 rpm for 2 h (running for 10 min and pausing for 2 min) with the ball to powder mass ratio of 50 : 1. These semi-finished products absorbed hydrogen again at 300 °C, 5 MPa for 10 h. After cooled down, these products were processed for longer ball milling for 6 h (running for 6 min and pausing for 6 min) at a speed of 400 rpm with the ball to powder mass ratio of 50 : 1. The final product is denoted as MgH2+CeF3@Gn. For comparison, the contrast samples MgH_2+Gn, MgH_2+CeF_3 and undoped MgH_2 were prepared under the same conditions.

Phase structures were determined by powder X-ray diffraction (XRD) using a Bruker-D8 ADVANCE X-ray diffractometer with Co Kα (λ = 1.7902 Å) radiation. When the samples were transferred and measured, they were sealed with amorphous membranes to prevent oxidation. Scanning electron microscope (SEM, Hitachi SU-8010) was employed to observe the morphologies of the samples. Raman spectrum (LabRAM HR Evolution, excitation 532 nm). Differential scanning calorimetry (DSC, Netzsch, STA449F5) was used to calculate the apparent activation energies of dehydrogenation. The samples were heated from room temperature to 500 °C at a rate of 2 °C/min, 4 °C/min, 8 °C/min,16 °C/min respectively. Before heated, the sample was vacuumed and during the heating process, argon was owed at 50 mL min^{-1} to prevent sample oxidation.

Quantitative measurements of the hydrogen desorption and absorption were carried out on a homemade Sieverts-type apparatus. The onset hydrogen desorption temperature and hydrogen desorption capacity were analyzed through temperature-programmed desorption (TPD) at a heating rate of 2 °C/min. To analyze the hydrogen desorption/absorption kinetics properties, the isothermal desorption measurements were carried out at different temperatures (dehydrogenation at 250 °C, 275 °C, 300 °C under vacuum, and hydrogenation at 250 °C, 200 °C, 150 °C under 3 MPa hydrogen pressure, respectively). Before the temperature reached the set value, filled 5 MPa hydrogen to prevent the sample from dehydrogenation. All handling of these samples were carried out in a glovebox (MIKROUNA) filled with a high purity argon and maintain oxygen and water vapor contents lower than 1 ppm. It's noteworthy that all samples absorb hydrogen at 300 °C under 5 MPa hydrogen pressure for 30 min before desorption measurements.

Results and discussion

Microstructures

XRD and Raman spectra patterns of raw Gn, the treated Gn (which were only treated with concentrated nitric acid) and CeF_3@Gn are shown in Fig. 1. As shown in Fig. 1(a), it can be clearly seen that the diffraction peaks in the XRD patterns are all consistent with the standard peaks of C and CeF_3. It indicates the pure additives were successfully obtained. Moreover, the Raman spectra was carried out to confirm the fact that the treated Gn is superior to raw Gn when used as an additive, as shown in Fig. 1(a). Raman spectra display D, G, 2D and D + G peaks at around 1343, 1580, 2454, 2721 cm^{-1}, that correspond to some of the literature [41,53–55], and a widespread agreement is that D peak can be expressed as sp3 hybridization, G peak can be assigned to sp2 hybridization, 2D

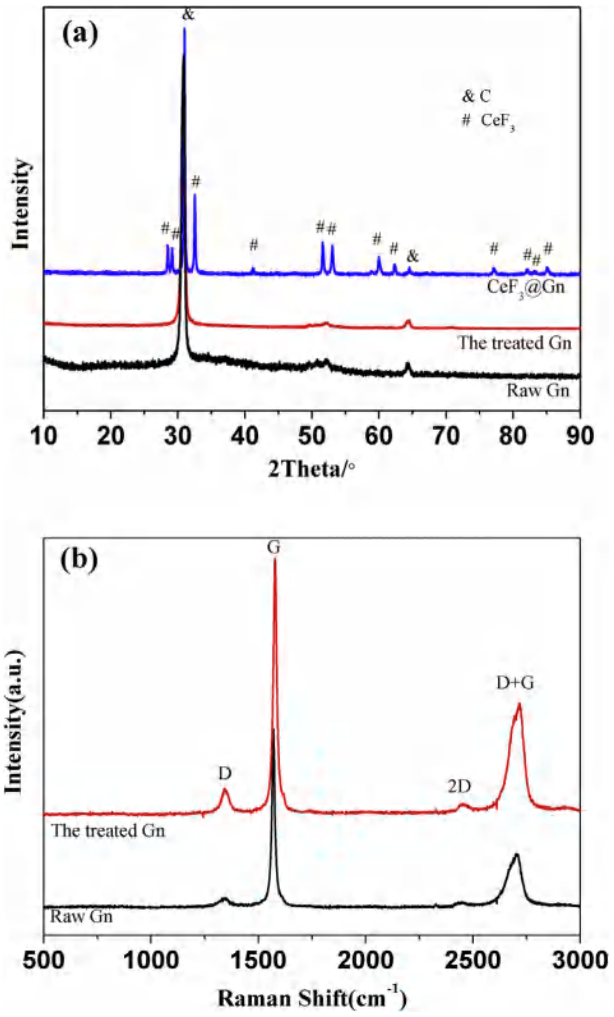

Fig. 1 – XRD and Raman spectra patterns of the raw Gn, the treated Gn (which were only treated with concentrated nitric acid) and CeF_3@Gn.

peak is used for judging layers of graphene and D + G peak can be used to illustrate the defects in graphene [54,55]. So, the intensity ratio of D + G for the treated Gn (which was only treated with concentrated nitric acid) showed a little better value than raw Gn.

Furthermore, the morphological features of the raw Gn, the treated Gn and CeF_3@Gn were clearly characterized using SEM, and the results are presented in Fig. 2, respectively. The confusion degree of graphene was increased after treatment with concentrated nitric acid by comparing Fig. 2(a and b), which is beneficial to the dispersion of CeF_3 nano-particles on its surface. And from Fig. 2(c), we can see that CeF_3 nano-particles are uniformly dispersed on the Gn surface.

Fig. 3 shows XRD patterns of the as-prepared Mg + CeF_3@-Gn and contrast samples which have already absorbed hydrogen at 300 °C under 5 MPa hydrogen pressure for 30 min. It is clearly shown that no diffraction peaks corresponding to Mg are detected for MgH_2+CeF_3@Gn, but for the contrast samples the diffraction peaks corresponding to Mg are detected, and the MgH_2 diffraction peaks of MgH_2+CeF_3@Gn are broader and weaker, indicating the increase of lattice strain and the reduction of grain size. It is well known that the decreased grain size may shorten the hydrogen diffusion channel, which is beneficial for improving kinetics performance [56]. Diffraction peaks corresponding to CeH_{2-3} also exist in the hydrogenated samples (MgH_2+CeF_3@Gn and MgH_2+CeF_3), which suggests that CeF_3 may have reacted with MgH_2, Mg and hydrogen during the hydrogen desorption process, and form CeH_{2-3}. Mg still exists in the contrast samples means that hydrogen absorption is incomplete, which results in the reduction of hydrogen storage capacity.

SEM was employed to observe the surface morphology of the samples, and the results are shown in Fig. 4, from which it can be seen that many small and inhomogeneous particles adhere to the surface of the large particles, especially for MgH_2+CeF_3@Gn. And Gn dispersed in a state of disorder and

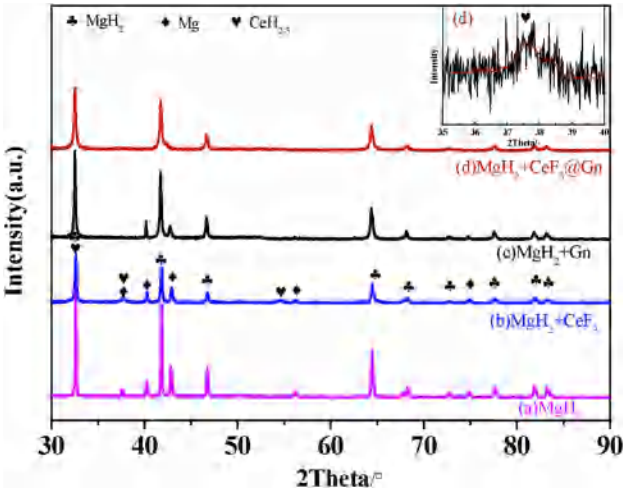

Fig. 3 – The XRD patterns of as-prepared MgH_2+CeF_3@Gn, MgH_2+CeF_3, MgH_2+Gn, and undoped MgH_2 after hydrogen absorption for 30 min.

irregular after ball milling, which helps to reduce particle size and serves as "hydrogen diffusion channel".

In order to study the distribution of elements in CeF_3@Gn and MgH_2+CeF_3@Gn, EDS mapping analyses were performed, as shown in Fig. 5. From Fig. 5(a), it can be seen that uniformly dispersed CeF_3 located on the surface of graphene nanoplates, and the distribution of C and Ce and F shown in Fig. 5(b) reveals the catalyst was uniformly distributed in MgH_2. These prove that wet method ball milling and hydriding treatment are effective way to add the dispersion of additives on MgH_2 matrix.

Hydrogen desorption/absorption performance

Fig. 6(a) shows the TPD (temperature programmed desorption) curves for the four samples. Vertical coordinate represents the

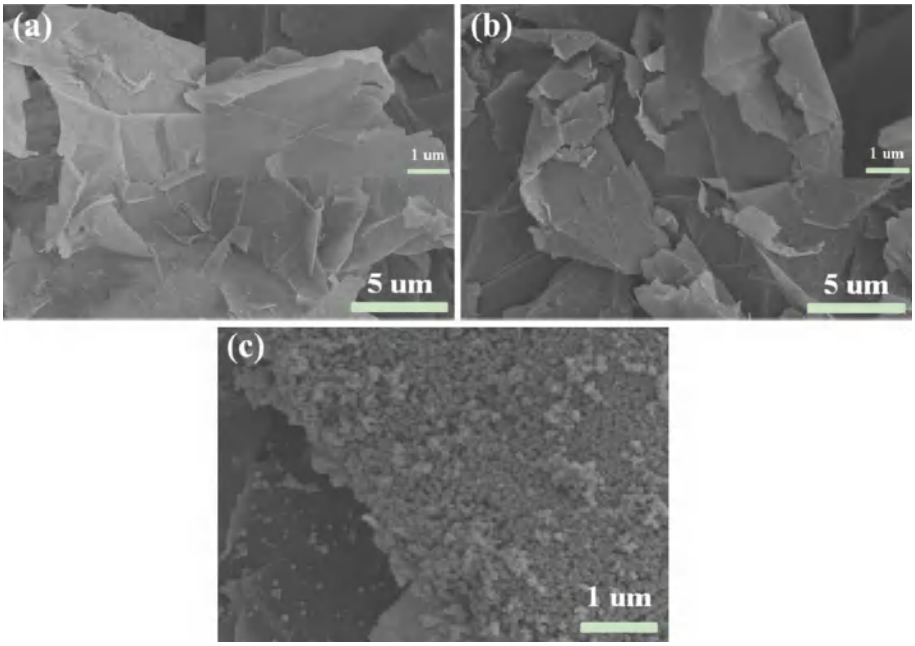

Fig. 2 – SEM of raw Gn, the treated Gn (which were only treated with concentrated nitric acid) and CeF_3@Gn.

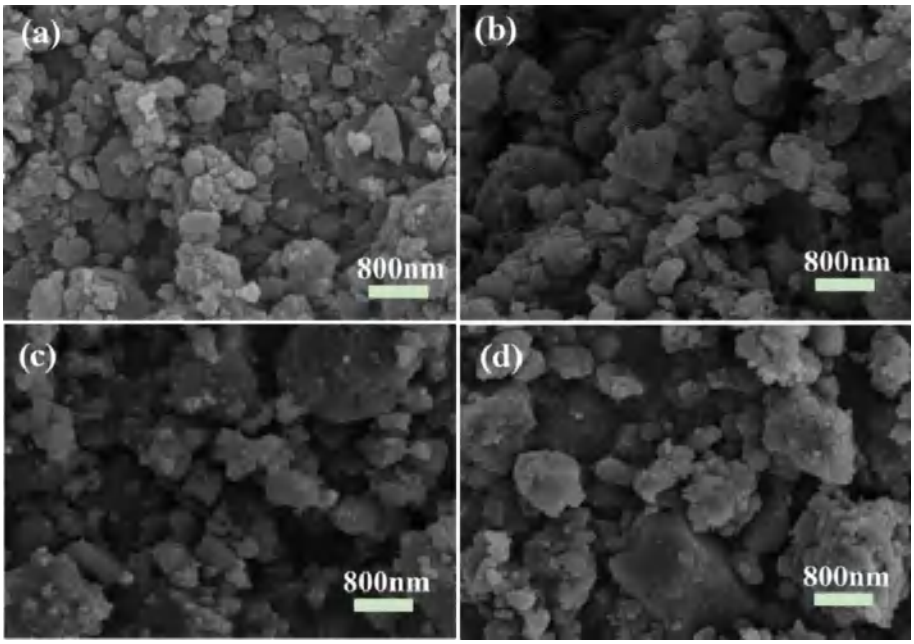

Fig. 4 – SEM images of the as-prepared samples: (a) MgH_2+CeF_3@Gn; (b) MgH_2+Gn; (c) MgH_2+CeF_3; (d) MgH_2.

percentage of hydrogen desorption, transverse coordinate represents the temperature of hydrogen desorption. When the curve of hydrogen desorption starts to deviate from 0 wt% and quick hydrogen releases, it corresponds the starting dehydrogenation point. So it can be seen that MgH_2+CeF_3@Gn starts to release hydrogen at around 232 °C, which is 86 °C lower than that of as-milled undoped MgH_2. We can see from Fig. 6(b) peak hydrogen release temperature is also reduced by 80 °C, so CeF_3@Gn can improved thermodynamic performance of MgH_2. And Fig. 6(a) shows the full dehydrogenation completed at around 310 °C for MgH_2+CeF_3@Gn, which is also 90 °C lower than that of as-milled MgH_2. The total amount of hydrogen release is about 6.77 wt%, which is 99% of its theoretical capacity (6.84 wt%). However, under the same conditions MgH_2+Gn and MgH_2+CeF_3 completely released hydrogen about 6.24 wt% (91.2%), 6.17 wt% (90.1%), respectively. And under the same conditions the onset hydrogen desorption temperature of the as-milled undoped MgH_2 is about 318 °C, and desorbed about 6.75 wt% after 400 °C , which is only 88.8% of theoretical capacity (7.6 wt%). The hydrogen desorption capacity of contrast samples is lower than the theoretical hydrogen capacity, the incomplete hydrogenation for these samples is also one of the reasons. This also agrees with the analysis results as shown in Fig. 3. Synergetic catalysis of CeF_3 and Gn (graphene) makes the sample generate more MgH_2 during the preparation process, and MgH_2 has good brittleness which is helpful to reduce the particle size during ball mill process and accelerates the absorption kinetics, so that the sample with CeF_3@Gn addition can be hydrided completely. But contrast samples cannot be fully hydrided.

To study the hydrogen desorption kinetics, isothermal hydrogen desorption measurements were performed. Fig. 7 shows the dehydrogenation kinetic curves of the four samples at 300 °C , 275 °C , 250 °C, respectively. As we can see from Fig. 7(a), under condition of 300 °C desorption, MgH_2+CeF_3@Gn can release 6.67 wt% hydrogen within 13 min , which is 97.5% of the theoretical hydrogen capacity, and the maximum hydrogen desorption rate is around 0.70 wt%H_2/min, which is 79.5 times faster than that of the as-milled undoped MgH_2 (the hydrogen desorption rate within the first 30 min under 300 °C is around 0.0088 wt%H_2/min). In contrast , MgH_2+CeF_3, MgH_2+Gn and MgH_2 only can release 2 wt%, 1.80 wt% and 0.19 wt% hydrogen under the same conditions, respectively.

Under desorption temperature of 275 °C, MgH_2+CeF_3@Gn, MgH_2+CeF_3, MgH_2+Gn and MgH_2 can release 6.35 wt%, 2.81 wt %, 2.08 wt% and 0.22 wt% hydrogen in 45 min, respectively. The maximum hydrogen desorption rate of the as-milled undoped MgH_2 is around 0.0038 wt%H_2/min, while that of MgH_2+CeF_3@Gn reached 0.2 wt%H_2/min, which is 52.6 times faster than the as-milled undoped MgH_2.

As the desorption temperature decreased to 250 °C, the as-milled undoped MgH_2 can hardly release hydrogen, its hydrogen desorption rate is only around 0.00067 wt% H_2/min. When CeF_3 and Gn is added, the hydrogen desorption rate increases remarkably, MgH_2+CeF_3, Mg + Gn release 0.75 wt% and 0.51 wt% hydrogen within 60 min, respectively. Mg + CeF_3@Gn shows the best hydrogen desorption properties. It can desorb 4.01 wt% and 5.32 wt% hydrogen within 60 min and 120 min, respectively. And the maximum hydrogen desorption rate still reached 0.079 wt%H_2/min, which is 118 times faster than that of the as-milled undoped MgH_2.

The hydrogen desorption kinetics was also investigated by DSC measurements. Fig. 8 shows the DSC curves performed at different heating rates (2 °C/min, 4 °C/min, 8 °C/min, 16 °C/min). And the apparent activation energy (E_a) of hydrogen release reaction was estimated by Kissinger's equation. The equation as follows:

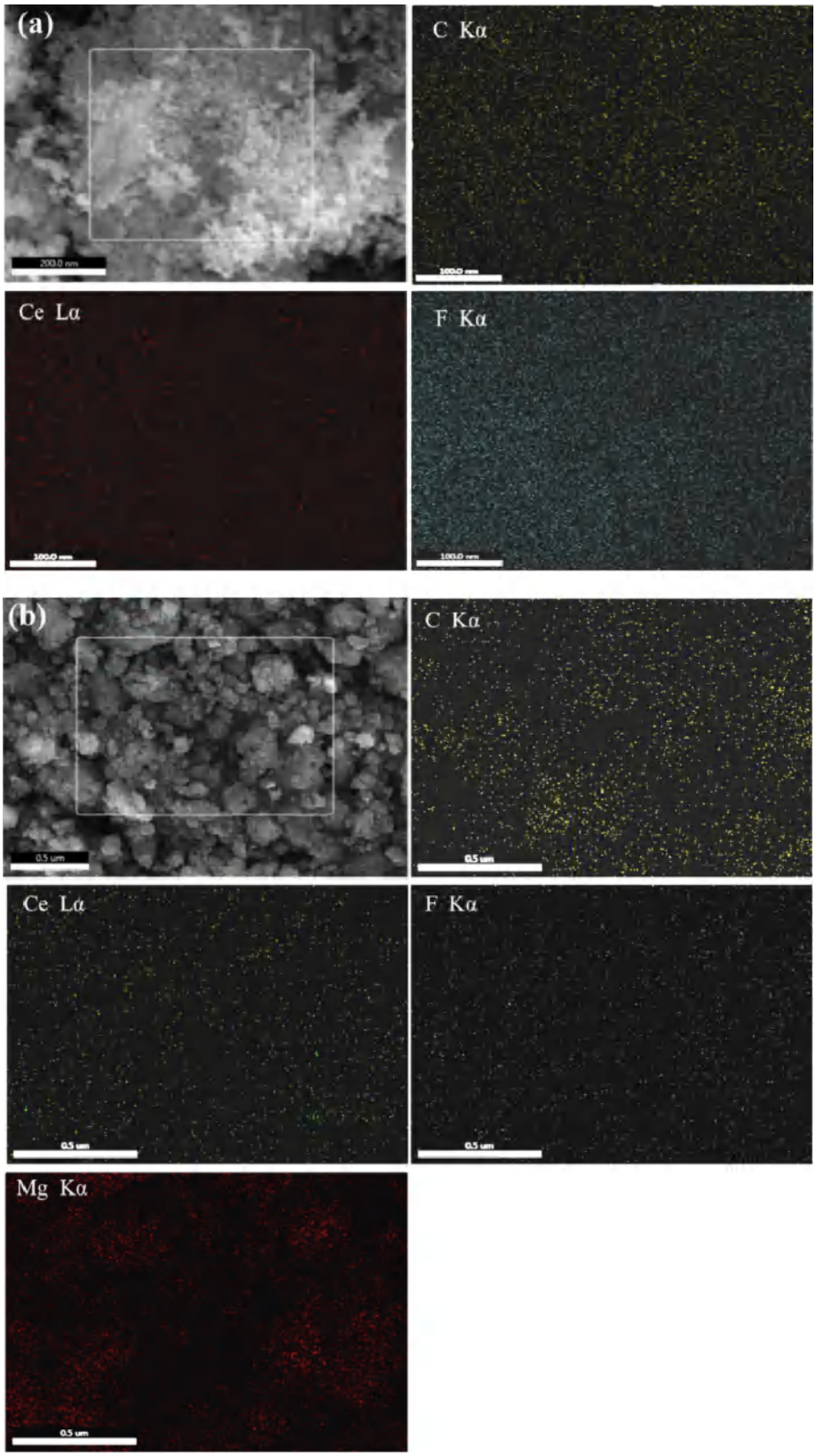

Fig. 5 – SEM image and EDS mapping of (a) CeF_3@Gn and (b) MgH_2+CeF_3@Gn.

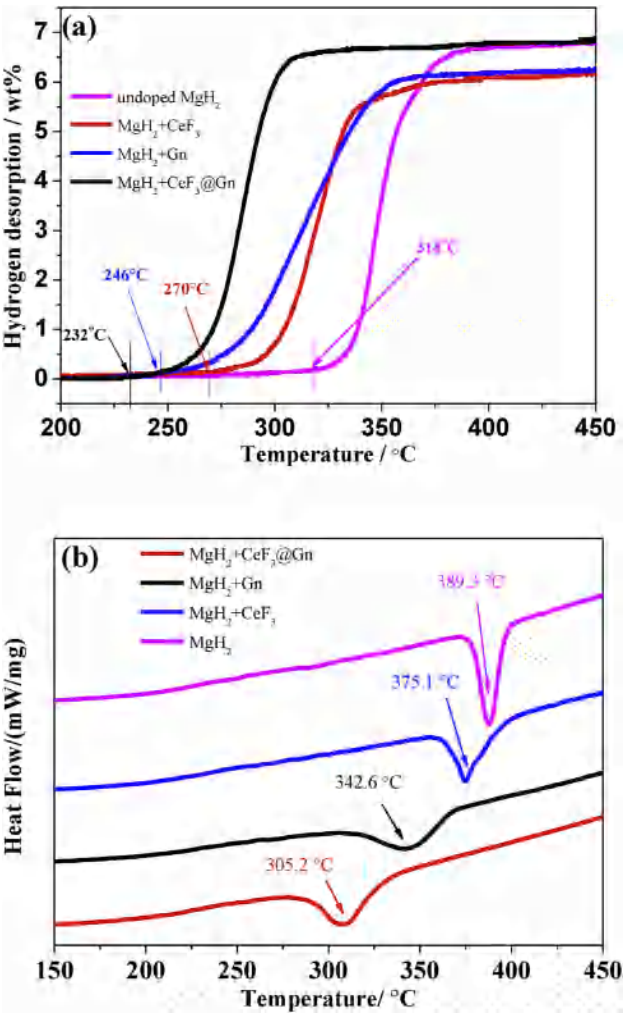

Fig. 6 – TPD and DSC curves of MgH_2+CeF_3@Gn and the contrast samples.

$$\ln\left(\beta \Big/ T_p^2\right) = -E_a / RT_p + A \quad (1)$$

where β is the heating rate (2 °C/min, 4 °C/min, 8 °C/min, 16 °C/min) and Tp is the peak temperature of hydrogen release, which can be got from Fig. 8. R is the ideal gas constant (8.314 J mol^{-1} K^{-1}). A is a constant. As shown in Fig. 9, the E_a can be calculated from the slope times R in a plot of ln (β/T_p^2) versus 1000/T_p. After fitting we got hydrogen desorption activation energy of the four samples. The apparent activation energy of MgH_2+CeF_3@Gn is around 128.7 kJ/mol, which was decreased by 76.7 kJ/mol compared to the undoped MgH_2, much better than those of MgH_2-10 wt%K_2TiF_6 [57], MgH_2-$FeCl_3$ and Carbon Nanotubes [46], as well as other composites [26,35,47,49]. And it is also lower than that of separately added samples. The results clearly show CeF_3@Gn, Gn and CeF_3 all can improve the dehydrogenation kinetics compared to the undoped MgH_2. Moreover, co-addition of Gn and CeF_3 shows synergistic effect on enhancing the hydrogen storage properties, which agrees with the results as shown in Fig. 8.

The hydrogen absorption behavior was studied for the samples after dehydrogenation. Fig. 10 shows the absorption kinetics of Mg + CeF_3@Gn and three other comparative

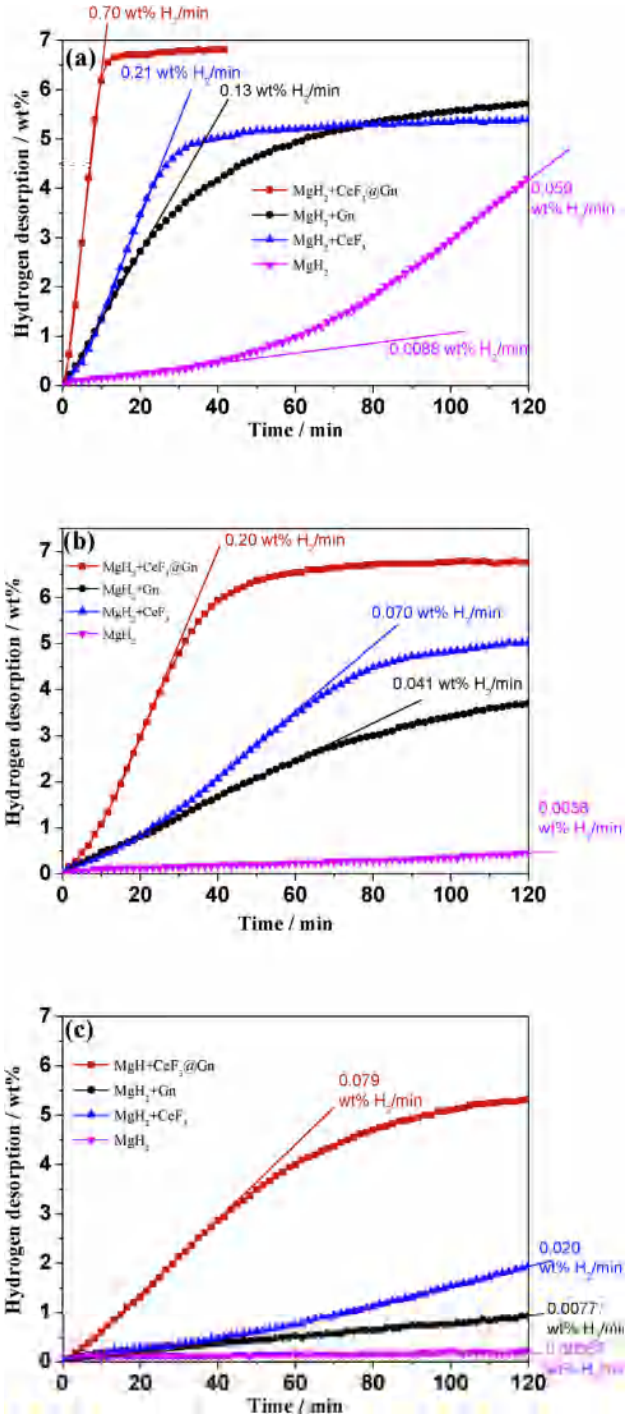

Fig. 7 – Isothermal hydrogen desorption curves of MgH_2+Gn@CeF_3 and contrast samples at (a) 300 °C (b) 275 °C (c) 250 °C.

samples at 250 °C, 200 °C, 150 °C and under hydrogen pressure of 3.0 MPa.

The results show that co-addition of CeF_3 and Gn would not only greatly increase the hydrogen absorption rate, but also increase the hydrogen absorption capacity. Mg + CeF_3@-Gn can absorb 6.52 wt% hydrogen within 50 s at 250 °C, the undoped Mg only absorbs 0.85 wt% under the same conditions. When the temperature decreased to 200 °C, the

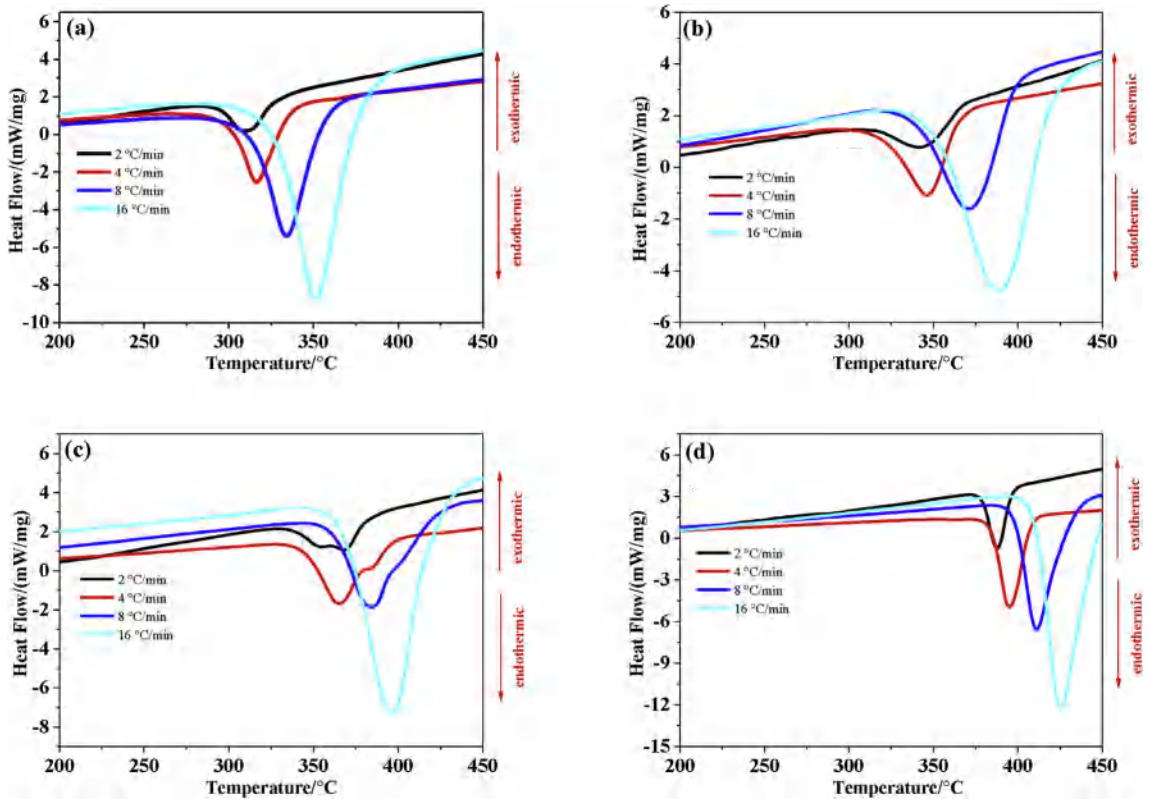

Fig. 8 – DSC curves at different heating rates (2 °C/min, 4 °C/min, 8 °C/min, 16 °C/min) for (a) MgH_2+CeF_3@Gn; (b) MgH_2+Gn; (c) MgH_2+CeF_3; (d) MgH_2.

undoped Mg only absorbs 0.15 wt% hydrogen within 50 s, while Mg + CeF_3@Gn still can absorb 6.23 wt% hydrogen within 50 s, which is one of the best hydrogen absorption rates at 200 °C for Mg-base material so far reported.

As the temperature further decreased to 150 °C, the undoped Mg can hardly absorb hydrogen, its hydrogen absorption rate is only 0.0085 wt%H_2/min, while Mg + CeF_3@Gn can absorb 5.71 wt% hydrogen within 50 s, its maximum hydrogen absorption rate reached 15.0 wt%H_2/min, which is 1765 times faster than that of the undoped Mg. At this low temperature, hydrogen absorption rate of Mg + Gn is also extremely slow (0.059 wt%H_2/min).

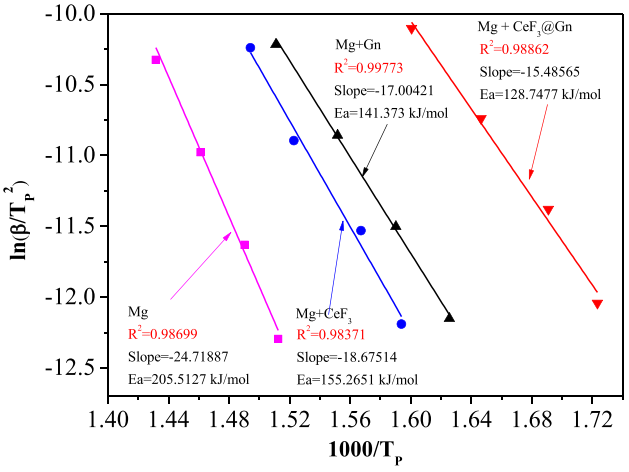

Fig. 9 – Kissinger plots for MgH_2+CeF_3@Gn and three other contrast samples.

The decomposition of hydrogen molecule on the sample surface and the diffusion of hydrogen atom into the bulk have great influence on the kinetics of re-hydrogenation performance. The addition of CeF_3 helps the decomposition of H_2 molecule [48,50], which is largely due to the action of the by-product of the reaction. Figs. 3 and 12 confirm the presence of MgF_2 and CeH_{2-3} after re-hydrogenation. Graphene helps shorten the diffusion path, but the effect of graphene on hydrogen absorption is not obvious at low temperature. Hence, the effect of co-addition of CeF_3 and Gn on hydrogen absorption performance is not simple superposition, but is great mutual promotion and synergistic catalysis.

The cycling properties of MgH_2+CeF_3@Gn were studied by measuring the isothermal hydrogen desorption at 300 °C for 1 h and hydrogen absorption at 300 °C under 5 MPa hydrogen pressure for 30 min. The results are shown in Fig. 11. It can be seen from Fig. 11 that no eminent decrease of hydrogen desorption capacity occurred in the 15 hydrogen desorption and absorption cycles, which indicates excellent cyclic stability. It is better than MgH_2+5 wt%NbF_5+5 wt%SWNTs , which about only 4.5 wt% hydrogen can be desorbed within 60 min at the first ten times hydrogen desorption and absorption [34] , and many composites show should not be neglected decrease during hydrogen desorption and absorption cycles [46,58].

XRD patterns of hydrogen absorption product after 15 cycles are shown in Fig. 12. The peaks related to MgH_2,

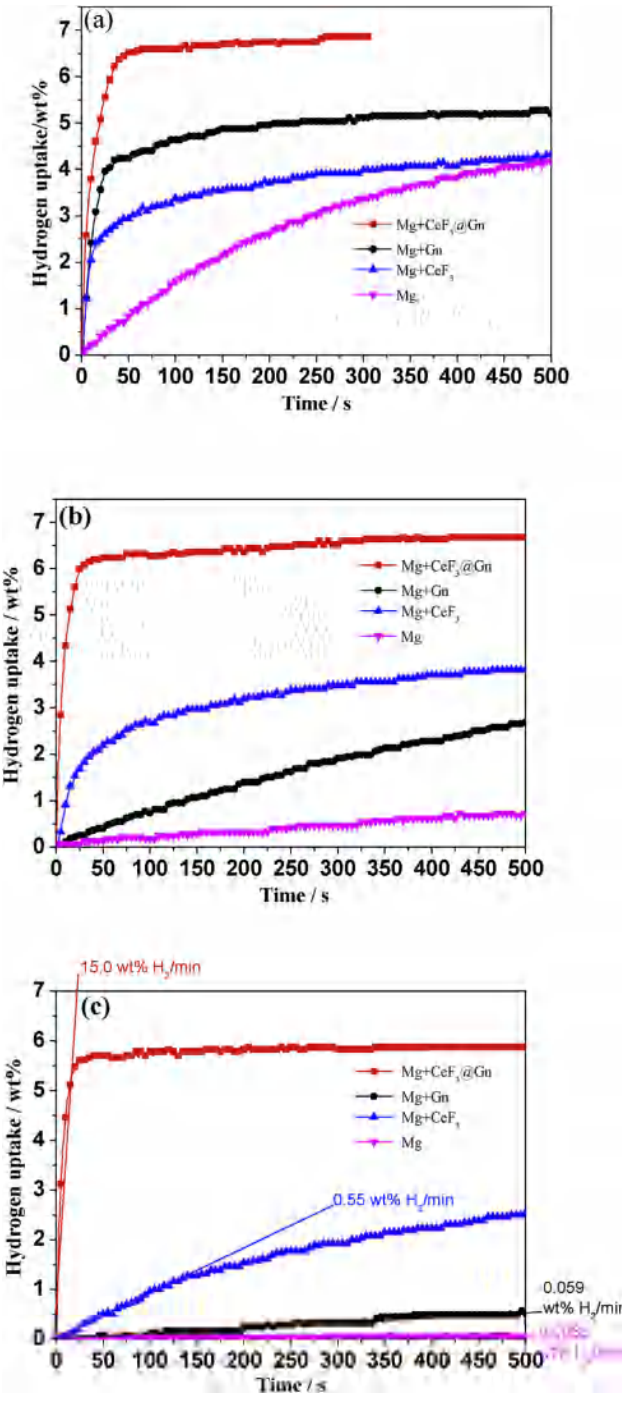

Fig. 10 – Isothermal re-hydriding curves of Mg + Gn@CeF_3 and contrast samples at (a) 250 °C (b) 200 °C (c) 150 °C.

unhydrided Mg, CeH_{2-3}, MgF_2 are detected. The in situ formed CeH_{2-3} and MgF_2 are cyclic stable, and they can effectively suppress Mg/MgH_2 grain growth and improves the hydrogen desorption and absorption properties of MgH_2. Many studies reported the by-product rare earth hydride remains during the desorption/absorption processes [50,51,58–60]. However, in this work, we found that the CeH_{2-3} was only found in the hydrided samples, and it disappeared after the sample was dehydrided, as shown in Fig. 13. CeH_{2-3} acts as "hydrogen

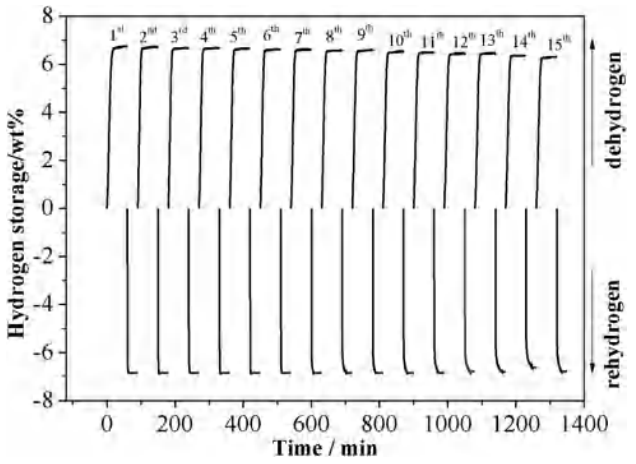

Fig. 11 – Isothermal de/re-hydrogenation cycling curves of MgH_2+CeF_3@Gn

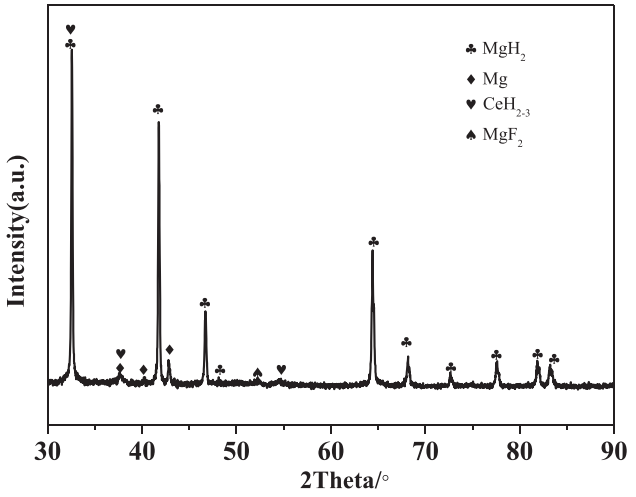

Fig. 12 – The XRD patterns of MgH_2+CeF_3@Gn after hydrogen absorption at 15th cycle.

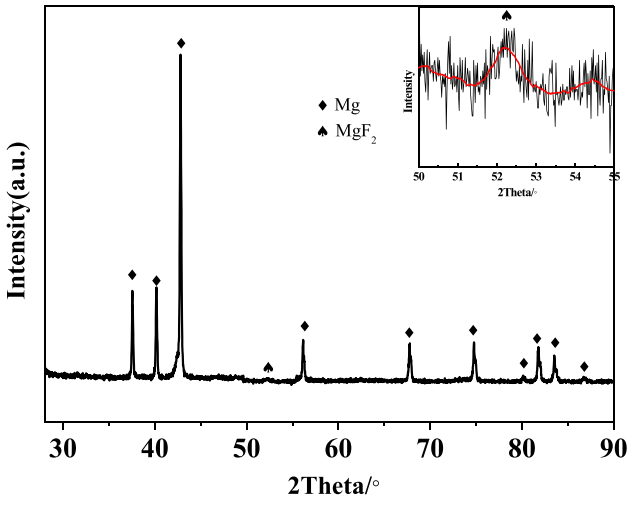

Fig. 13 – The XRD patterns of 300 °C isothermal hydrogen desorption sample of Mg + CeF_3@Gn.

pump effect", can weaken the stability of MgH_2, which helps to improve the performance of hydrogen release kinetics.

Conclusion

In conclusion, with wet method, ball milling and hydriding method we have prepared MgH_2+CeF_3@Gn, MgH_2+CeF_3, MgH_2+Gn and undoped MgH_2. The hydrogen storage behavior of the prepared samples were investigated. The onset hydrogen desorption temperature of MgH_2+CeF_3@Gn is 232 °C, which is 86 °C lower than as-milled undoped MgH_2. And the full dehydrogenation completed at around 310 °C for MgH_2+CeF_3@Gn, which is also 90 °C lower than that of as-milled MgH_2, and the hydrogen desorption capacity reaches 6.77 wt%, which is 99% of its theoretical capacity (6.84 wt%). At 300 °C and 200 °C the maximum hydrogen desorption rates are 79.5 and 118 times faster than that of the as-milled undoped MgH_2. After hydrogen desorption the CeF_3@Gn catalyzed Mg also showed excellent hydrogen absorption properties. Even at low temperature of 150 °C, Mg + CeF_3@Gn can absorb 5.71 wt% hydrogen within 50 s, and its maximum hydrogen absorption rate reached 15.0 wt%H_2/min, which is 1765 times faster than that of the undoped Mg. No eminent decrease of hydrogen storage capacity occurred after 15 hydrogen desorption/absorption cycles, which indicates excellent cyclic stability. Based on the superior the hydrogen storage properties, we believed the by-products of MgF_2 and CeH_{2-3} that were formed in situ during re/dehydrogenation, cooperate with the unique structure of Gn played a key role. In situ generation of products is an excellent method which shows mutually beneficial for overcoming the agglomeration and enhancing the thermodynamics and kinetics, this gives us a direction to synthesize additives of Mg-based hydrogen storage materials or other materials.

Acknowledgements

This work was supported by the National Natural Science Foundation of China (No.51771171 , and 51971199) and the Foundation of Education Department of Guangxi Zhuang Autonomous Region of China (No. 2019KY0021).

REFERENCES

[1] Sen B, Kuzu S, Demir E, Onal Okyay T, Sen F. Hydrogen liberation from the dehydrocoupling of dimethylamine–borane at room temperature by using novel and highly monodispersed RuPtNi nanocatalysts decorated with graphene oxide. Int J Hydrogen Energy 2017;42:23299–306.

[2] Sen B, Kuzu S, Demir E, Yıldırır E, Sen F. Highly efficient catalytic dehydrogenation of dimethyl ammonia borane via monodisperse palladium–nickel alloy nanoparticles assembled on PEDOT. Int J Hydrogen Energy 2017;42:23307–14.

[3] Sen B, Kuzu S, Demir E, Akocak S, Sen F. Highly monodisperse RuCo nanoparticles decorated on functionalized multiwalled carbon nanotube with the highest observed catalytic activity in the dehydrogenation of dimethylamine–borane. Int J Hydrogen Energy 2017;42:23292–8.

[4] Eris S, Daşdelen Z, Yıldız Y, Sen F. Nanostructured Polyaniline-rGO decorated platinum catalyst with enhanced activity and durability for Methanol oxidation. Int J Hydrogen Energy 2018;43:1337–43.

[5] Şen B, Aygün A, Okyay TO, Şavk A, Kartop R, Şen F. Monodisperse palladium nanoparticles assembled on graphene oxide with the high catalytic activity and reusability in the dehydrogenation of dimethylamine-borane. Int J Hydrogen Energy 2018;43:20176–82.

[6] Zhang Y, Zhang H, Ding X, Liu D, Zhang Q, Si T. Microstructure characterization and hydrogen storage properties study of $Mg_2Ni_{0.92}M_{0.08}$ (M = Ti, V, Fe or Si) alloys. Prog Nat Sci: Mater Int 2018;28:464–9.

[7] Jiang X, Wu Y, Fu K, Zheng J, Li X. Hydrogen storage properties of $LaMg_4Cu$. Intermetallics 2018;95:73–9.

[8] Ding X, Chen R, Chen X, Li X, Guo J, Su Y, et al. Dependence and mechanism of hydrogenation behavior on absorption conditions in hypo-eutectic Mg–Ni–Cu alloy. Int J Hydrogen Energy 2018;43:16617–22.

[9] Ning H, Zhou X, Zhang Z, Zhou W, Guo J. Ni catalytic effects for the enhanced hydrogenation properties of $Mg_{17}Al_{12}$(1 1 0) surface. Appl Surf Sci 2019;464:644–50.

[10] Wagemans RW, van Lenthe JH, Jongh PE, Van Dillen AJ, de Jong KP. Hydrogen storage in magnesium clusters: quantum chemical study. J Am Chem Soc 2005;127(47):16675–80.

[11] Norberg NS, Arthur TS, Fredrick SJ, Prieto AL. Size-dependent hydrogen storage properties of Mg nanocrystals prepared from solution. J Am Chem Soc 2011;133:10679–81.

[12] Li W, Li C, Ma H, Chen J. Magnesium nanowires: enhanced kinetics for hydrogen absorption and desorption. J Am Chem Soc 2007;129(21):6710–1.

[13] Zhang T, Hou X, Hu R, Kou H, Li J. Non-isothermal synergetic catalytic effect of TiF_3 and Nb_2O_5 on dehydrogenation high-energy ball milled MgH_2. Mater Chem Phys 2016;183:65–75.

[14] Liu Z, Lei Z. Cyclic hydrogen storage properties of Mg milled with nickel nano-powders and MnO_2. J Alloy Comp 2007;443:121–4.

[15] Hanada N, Ichikawa T, Hino S, Fujii H. Remarkable improvement of hydrogen sorption kinetics in magnesium catalyzed with Nb_2O_5. J Alloy Comp 2006;420:46–9.

[16] ullah Rather S, Taimoor AA, Muhammad A, Alhamed YA, Zaman SF, Ali AM. Kinetics of hydrogen adsorption on MgH_2/CNT composite. Mater Res Bull 2016;77:23–8.

[17] Fan X, Xiao X, Chen L, Wang X, Li S, Ge H, et al. High catalytic efficiency of amorphous TiB_2 and NbB_2 nanoparticles for hydrogen storage using the $2LiBH_4$–MgH_2 system. J Mater Chem 2013;1:11368.

[18] Mo X, Jiang W. Dehydrogenation properties of $LiBH_4$ modified by Mg from first-principles calculations. J Alloy Comp 2018;735:668–76.

[19] Liu BH, Zhang BJ, Jiang Y. Hydrogen storage performance of $LiBH_4$+1/2MgH_2 composites improved by Ce-based additives. Int J Hydrogen Energy 2011;36:5418–24.

[20] Ma M, Ouyang L, Liu J, Wang H, Shao H, Zhu M. Air-stable hydrogen generation materials and enhanced hydrolysis performance of MgH_2-$LiNH_2$ composites. J Power Sources 2017;359:427–34.

[21] Ouyang LZ, Cao ZJ, Wang H, Liu JW, Sun DL, Zhang QA, et al. Dual-tuning effect of in on the thermodynamic and kinetic properties of Mg_2Ni dehydrogenation. Int J Hydrogen Energy 2013;38:8881–7.

[22] Ouyang L, Cao Z, Wang H, Hu R, Zhu M. Application of dielectric barrier discharge plasma-assisted milling in energy storage materials – a review. J Alloy Comp 2017;691:422–35.

[23] Ouyang LZ, Cao ZJ, Wang H, Liu JW, Sun DL, Zhang QA, et al. Enhanced dehydriding thermodynamics and kinetics in Mg(In)–MgF_2 composite directly synthesized by plasma milling. J Alloy Comp 2014;586:113–7.
[24] Yahya MS, Ismail M. Catalytic effect of SrTiO3 on the hydrogen storage behaviour of MgH_2. J Energy Chem 2019;28:46–53.
[25] Juahir N, Mustafa NS, Sininb AM, Ismail M. Improved hydrogen storage properties of MgH_2 by addition of Co_2NiO nanoparticles. RSC Adv 2015;5:60983–9.
[26] Sulaiman NN, Juahir N, Mustafa NS, Halim Yap FA, Ismail M. Improved hydrogen storage properties of MgH_2 catalyzed with K_2NiF_6. J Energy Chem 2016;25:832–9.
[27] Yahya MS, Ismail M. Synergistic catalytic effect of $SrTiO_3$ and Ni on the hydrogen storage properties of MgH_2. Int J Hydrogen Energy 2018;43:6244–55.
[28] Mustafa NS, Sulaiman NN, Ismail M. Effect of $SrFe_{12}O_{19}$ nanopowder on the hydrogen sorption properties of MgH_2. RSC Adv 2016;6:110004–10.
[29] Ismail M, Mustafa NS, Ali NA, Sazelee NA, Yahya MS. The hydrogen storage properties and catalytic mechanism of the $CuFe_2O_4$-doped MgH_2 composite system. Int J Hydrogen Energy 2019;44:318–24.
[30] Cui J, Liu J, Wang H, Ouyang L, Sun D, Zhu M, et al. Mg–TM (TM: Ti, Nb, V, Co, Mo or Ni) core–shell like nanostructures: synthesis, hydrogen storage performance and catalytic mechanism. J Mater Chem 2014;2:9645–55.
[31] Kang S, Klebanoff LE, Baker AA, Cowgill DF, Stavila V, Lee JRI, et al. Assessing the reactivity of $TiCl_3$ and TiF_3 with hydrogen. Int J Hydrogen Energy 2018;43:14507–19.
[32] Xie L, Liu Y, Wang YT, Zheng J, Li XG. Superior hydrogen storage kinetics of MgH_2 nanoparticles doped with TiF3. Acta Mater 2007;55:4585–91.
[33] Kumar S, Singh PK, Rao GVSN, Kojima Y, Kain V. Synergic effect of vanadium trichloride on the reversible hydrogen storage performance of the Mg MgH_2 system. Int J Hydrogen Energy 2018;43:15330–7.
[34] Luo Y, Wang P, Ma L-P, Cheng H-M. Enhanced hydrogen storage properties of MgH_2 co-catalyzed with NbF_5 and single-walled carbon nanotubes. Scr Mater 2007;56:765–8.
[35] Ismail M. Influence of different amounts of $FeCl_3$ on decomposition and hydrogen sorption kinetics of MgH_2. Int J Hydrogen Energy 2014;39:2567–74.
[36] Ismail M, Mustafa NS, Juahir N, Yap FAH. Catalytic effect of $CeCl_3$ on the hydrogen storage properties of MgH_2. Mater Chem Phys 2016;170:77–82.
[37] De Castro JF, Yavari AR, LeMoulec A, Ishikawa TT. Improving H-sorption in MgH_2 powders by addition of nanoparticles of transition metal fluoride catalysts and mechanical alloying. J Alloy Comp 2005;389:270–4.
[38] Singh MK, Bhatnagar A, Pandey SK, Mishra PC, Srivastava ON. Experimental and first principle studies on hydrogen desorption behavior of graphene nanofibre catalyzed MgH_2. Int J Hydrogen Energy 2017;42:960–8.
[39] Soni PK, Bhatnagar A, Shaz MA, Srivastava ON. Effect of graphene templated fluorides of Ce and La on the de/rehydrogenation behavior of MgH_2. Int J Hydrogen Energy 2017;42:20026–35.
[40] Zhang J, Zhu Y, Zang X, Huan Q, Su W, Zhu D, et al. Nickel-decorated graphene nanoplates for enhanced H_2 sorption properties of magnesium hydride at moderate temperatures. J Mater Chem 2016;4(7):2560–70.
[41] Liu G, Wang Y, Xu C, Qiu F, An C, Li L, et al. Excellent catalytic effects of highly crumpled graphene nanosheets on hydrogenation/dehydrogenation of magnesium hydride. Nanoscale 2013;5:1074–81.
[42] Liu G, Wang Y, Qiu F, Li L, Jiao L, Yuan H. Synthesis of porous Ni@rGO nanocomposite and its synergetic effect on hydrogen sorption properties of MgH_2. J Mater Chem 2012;22:22542.
[43] Liu G, Wang Y, Jiao L, Yuan H. Understanding the role of few-layer graphene nanosheets in enhancing the hydrogen sorption kinetics of magnesium hydride. ACS Appl Mater Interfaces 2014;6:11038–46.
[44] Yahya MS, Ismail M. Improvement of hydrogen storage properties of MgH_2 catalyzed by K_2NbF_7 and multiwall carbon nanotube. J Phys Chem C 2018;122:11222–33.
[45] Sulaiman NN, Ismail M. Enhanced hydrogen storage properties of MgH_2 co-catalyzed with K_2NiF_6 and CNTs. Dalton Trans 2016;45:19380–8.
[46] Ismail M, Juahir N, Mustafa NS. Improved hydrogen storage properties of MgH_2 Co-doped with $FeCl_3$ and carbon nanotubes. J Phys Chem C 2014;118:18878–83.
[47] Gao S, Liu H, Xu L, Li S, Wang X, Yan M. Hydrogen storage properties of nano-CoB/CNTs catalyzed MgH_2. J Alloy Comp 2018;735:635–42.
[48] Sagawa M, Fujimura S, Togawa N, Yamamoto H, Matsuura Y. New material for permanent magnets on a base of Nd and Fe (invited). J Appl Phys 1984;55:2083–7.
[49] Ismail M. Effect of $LaCl_3$ addition on the hydrogen storage properties of MgH_2. Energy 2015;79:177–82.
[50] Ouyang LZ, Yang XS, Zhu M, Liu JW, Dong HW, Sun DL, et al. Enhanced hydrogen storage kinetics and stability by synergistic effects of in situ formed $CeH_{2.73}$ and Ni in $CeH_{2.73}$-MgH_2-Ni nanocomposites. J Phys Chem C 2014;118:7808–20.
[51] Lin H-J, Tang J-J, Yu Q, Wang H, Ouyang L-Z, Zhao Y-J, et al. Symbiotic $CeH_{2.73}/CeO_2$ catalyst: a novel hydrogen pump. Nano Energy 2014;9:80–7.
[52] Chong L, Zou J, Zeng X, Ding W. Effects of La fluoride and La hydride on the reversible hydrogen sorption behaviors of $NaBH_4$: a comparative study. J Mater Chem 2014;2:8557–70.
[53] Meng X, Wan C, Wang Y, Ju X. Porous Ni@C derived from bimetallic Metal–Organic Frameworks and its application for improving LiBH4 dehydrogenation. J Alloy Comp 2018;735:1637–47.
[54] TUINSTRA F, KOENIG JL. Raman spectrum of graphite. J Chem Phys 1970;53:1126.
[55] Kudin KN, Ozbas B, Schniepp HC, Prud'homme RK, Aksay IA, Car R. Raman spectra of graphite oxide and functionalized graphene sheets. Nano Lett 2007;8:36–41.
[56] Ouyang LZ, Ye SY, Dong HW, Zhu M. Effect of interfacial free energy on hydriding reaction of Mg–Ni thin films. Appl Phys Lett 2007;90:021917.
[57] Mustafa NS, Ismail M. Influence of K_2TiF_6 additive on the hydrogen sorption properties of MgH_2. Int J Hydrogen Energy 2014;39:15563–9.
[58] Liu H, Wu C, Zhou H, Chen T, Liu Y, Wang X, et al. Synergistically thermodynamic and kinetic tailoring of the hydrogen desorption properties of MgH_2 by co-addition of AlH3 and CeF_3. RSC Adv 2015;5(28):22091–6.
[59] Shang C, Guo Z. Structural and desorption characterisations of milled (MgH_2+Y,Ce)(MgH_2+Y,Ce) powder mixtures for hydrogen storage. Int J Hydrogen Energy 2007;32:2920–5.
[60] Mustafa NS, Ismail M. Hydrogen sorption improvement of MgH_2 catalyzed by CeO_2 nanopowder. J Alloy Comp 2017;695:2532–8.